

Contrast independence of dynamic random dot correlogram evoked VEP amplitude

Katalin Markó

Institute of Physiology,
Medical School University of Pécs,
Pécs, Hungary



Huba J. M. Kiss

Institute of Physiology,
Medical School University of Pécs,
Pécs, Hungary



Eszter Mikó-Baráth

Institute of Physiology,
Medical School University of Pécs,
Pécs, Hungary



Orsolya Bártfai

Department of Ophthalmology,
Medical School University of Pécs,
Pécs, Hungary



Béla Török

Department of Ophthalmology,
Kantonsspital St. Gallen,
St. Gallen, Switzerland



Ilona Kovács

Department of Cognitive Science,
University of Technology and Economics,
Budapest, Hungary



Gábor Jandó

Institute of Physiology,
Medical School University of Pécs,
Pécs, Hungary



Dynamic random dot correlograms (DRDCs) are binocular stimuli that evoke a percept and a visual evoked potential (VEP) only in case of a mature and functional binocular system. DRDC-VEP is a method extensively used to study cortical binocularity in human infants and nonverbal children. Although the DRDC-VEP was invented 3 decades ago, neither the fundamental parameters, including contrast, of the stimulation nor the cerebral processing mechanisms have been clarified. The objective of the present study was to investigate the variability and detectability of adults' VEPs to DRDC under different stimulus contrast conditions. DRDCs were presented on the red and green channels of a computer monitor and were viewed with red-green goggles. The steady state DRDC-VEPs were recorded in healthy adult volunteers, and response reliability was assessed by the T_{circ}^2 statistic. DRDC-VEP amplitude was independent of contrast, while VEP phases showed a weak correlation with contrast. Contrast invariance of DRDC-VEP amplitude suggests a very high contrast gain and dominant magnocellular input to the binocular correlation processing system.

Keywords: dynamic random dot correlogram, VEP, binocular vision, stereopsis, contrast gain, contrast sensitivity, binocular correlation/anti-correlation

Citation: Markó, K., Kiss, H. J. M., Mikó-Baráth, E., Bártfai, O., Török, B., Kovács, I., & Jandó, G. (2009). Contrast independence of dynamic random dot correlogram evoked VEP amplitude. *Journal of Vision*, 9(4):8, 1–10, <http://journalofvision.org/9/4/8/>, doi:10.1167/9.4.8.

Introduction

Brain electrical responses evoked by cyclopean stimuli were first studied in the late seventies (Lehmann & Julesz,

1978). Dynamic random dot correlograms (DRDC) (Julesz, Kropfl, & Petrig, 1980) are preferred stimuli in visual evoked potential (VEP) experiments. These binocular stimuli consist of a correlated and an anti-correlated phase and as they alternate, a pulsation is perceived. The

occipital VEP response is synchronous with the perceptual pulsation in case of an intact and mature binocular system. This technique is one of the simplest and most frequently used methods to detect functional cortical binocularity in nonverbal humans (Braddick et al., 1980; Eizenman et al., 1999; Petrig, Julesz, Kropfl, Baumgartner, & Anliker, 1981) and animals (Miezin, Myerson, Julesz, & Allman, 1981). Unlike dynamic random dot stereograms (DRDS), DRDCs are not sensitive to head alignment, and convergence movements of the eyes are not initiated (Julesz et al., 1980). The VEP response to cyclopean stimuli is absent if the stimulus is viewed monocularly or if the subject has no functional binocular vision. DRDC-VEPs have also been used to determine the onset ages for cortical fusion and stereopsis in infants (Birch & Petrig, 1996; Braddick et al., 1980; Petrig et al., 1981).

Although the DRDC-VEP was invented three decades ago, its dependence on fundamental stimulus parameters, such as contrast, has never been examined systematically, and the cerebral processing mechanisms of its VEP response have not been clarified either.

In 1903, Worth created a functional model for binocular vision, which has become a widely accepted useful clinical tool to describe the binocular status of strabismic and/or amblyopic patients. Worth established three hierarchically organized stages of binocular vision: (1) simultaneous perception, (2) binocular fusion, and (3) stereopsis (Worth, 1903). There is clinical evidence for the existence of selective impairments of these functions which can be measured with the Worth 4-dot test. Although the clinical relevance of the model is apparent (Morale et al., 2002), the neurophysiological background of his three stage model is far from understood.

According to the classic theory described by Livingstone and Hubel (1987), only the magnocellular (MC) channel is involved in the processing of stereoscopic depth, and the contribution of parvocellular (PC) structures could be neglected. However, psychophysical research has demonstrated that PC stream mediated cues (e.g., color information) help in solving the binocular matching problem in complex images (den Ouden, van Ee, & de Haan, 2005).

MC neurons have higher firing rates to luminance contrast than do neurons in the PC pathway. MC neurons react nonlinearly to contrast, whereas PC units show almost linear characteristics. The contrast gain of a typical MC neuron is about 10 times higher than that of PC neurons and their contrast response function usually saturates at lower contrasts (Kaplan & Shapley, 1982; Shapley, Kaplan, & Soodak, 1981). The amplitude of a luminance contrast evoked VEP is often linearly related to the log of contrast (Campbell & Maffei, 1970); however, these contrast amplitude response curves (CR) evoked by different spatial frequency gratings show some nonlinearities. Several authors have reported either a straight-line relation at low contrast followed by saturation at high contrast or a double-slope straight-line relation in their

studies (Bobak, Bodis-Wollner, Harnois, & Thornton, 1984; Rudvin, Valberg, & Kilavik, 2000; Valberg & Rudvin, 1997). These nonlinearities or multi-slope CRs can be associated with different parallel visual pathway sensitivities (Souza, Gomes, Saito, da Silva Filho, & Silveira, 2007). Sinusoidally modulated 11-Hz grating stimulation (MC dominant stimulus) showed high sensitivity to contrast, the best fit to the CR was the sigmoid function leveling off at around 30% (Alexander, Rajagopalan, Seiple, Zemon, & Fishman, 2005).

Stereoscopic depth processing mechanisms are affected by contrast. Stereoacuity improves with increasing contrast, unless the increase is monocular (Cormack, Stevenson, & Schor, 1991; Halpern & Blake, 1988; Legge & Gu, 1989). Interocular differences in contrast rapidly deteriorate binocular fusion, whereas equalizing interocular contrast restores it. This phenomenon is often referred to as contrast paradox in stereopsis (Stevenson & Cormack, 2000). Binocular cortical neurons are also modulated by contrast. Striate neurons linearly integrate contrast information yielding in binocular summation of contrast signals (Smith, Chino, Ni, & Cheng, 1997).

Studying CR of the DRDC-VEP is important, because (1) it provides insight into the behavior of the response and the processing mechanisms of binocular correlation and (2) it can suggest subcortical pathway (i.e., MC or PC) origins for cortical binocular information processing network.

Methods

Subjects

A total of 16 adult subjects (mean age: 25.7) were studied. Subjects were fully informed and signed a consent form before the experiment. All subjects had a routine vision screening and had normal or corrected-to-normal visual acuity. They presented normal stereovision in a psychophysical stereo vision test (for details, see Appendix A).

Stimuli and test protocols

Stimuli were generated on a standard personal computer and presented on the red and green channels of a 19-inch cathode ray tube computer monitor (Samsung Model 957 MB) with 320×240 pixels spatial and 60-Hz temporal resolution under eight different contrast conditions, while the space-average mean luminance among the levels was kept constant at 2.89 ± 0.18 cd/m². For dichoptic viewing, R26 low-pass (red) and YG09 band-pass (green) gelatin filters (Tóbiás Optic Ltd., Budapest, Hungary) were used. For filter and other technical details see Appendix A. The

lowest and highest contrast was the minimum/maximum attainable value with the given 24 bits video adapter/monitor/filter combination. Subjects viewed the screen binocularly from 100 cm through natural pupils and the red-green goggles.

Dynamic random dot correlogram

The DRDC stimulus has two alternating phases. In the correlated phase, random dot images consist of 50% dark (black) and 50% bright (yellow) dots, which are identical within the red and green channels. In the anti-correlated phase, images are composed of 50% red and 50% green dots; therefore, dark dots in the green channel correspond to every bright dot in the red and vice versa (for details, see [Appendix A](#)). Random dot images were updated 60 times per second. The image change was synchronized to the monitor refresh cycle. In each phase, 16 different correlated or anti-correlated images were presented, so the DRDC stimulus frequency was 1.875 Hz ($1/(2 * 16 * (1/60))$). One pixel subtended 7.5 min of arc. This pixel size was chosen because it is comparable with the literature (Birch & Petrig, 1996; Julesz et al., 1980).

The percept of a correlated phase is a noisy surface in the plane of the monitor, a sort of “snowstorm” while during anti-correlated frames “woolly” depth can be perceived (Julesz et al., 1980). Alternation between the two phases can only be detected by a person who has functional binocularity. The “woolly” depth and the “snowstorm” can be clearly seen below 0.5 Hz, at the 1.875-Hz stimulus rate the actual percept is a pulsation at this frequency.

Experimental procedure

Stimuli were presented in a random sequence of contrast levels. The presentation of the DRDC stimulus lasted for 70 s for each contrast level. Subjects were asked to fixate at the center of the monitor, avoid body movements, and report their perception between the runs. Subjects were allowed to rest or adjust their body position after each contrast level for 2–3 minutes, if required. Controls (see [Appendix A](#)) were performed at least at two randomly selected contrast levels for each subject.

Recording conditions and data analysis

Visual evoked potentials

Gold plated electrodes were placed conventionally at Fz and Oz with a ground electrode at Cz, corresponding to the ISCEV standard (Odom et al., 2004). Signals were sampled and processed with a CED 1401 Power (Cambridge Electronic Design Limited, Cambridge, England) data acquisition device. The electrical signals were amplified and band-pass filtered between 0.5 and 250 Hz, continuously sampled at 960 Hz, and stored with the

trigger pulses for off line analysis. The 960-Hz sampling rate was chosen in order to optimize parameters for the fast Fourier analysis used to extract the stimulus fundamental frequency and higher harmonics for further statistical analysis.

Analysis of DRDC-VEP

Raw EEG records were subdivided into 2.133 s non-overlapping epochs, i.e., 4 stimulus cycles or 2048 samples. Each epoch was FFT transformed, and the Fourier components of the stimulus fundamental frequency up to the 4th harmonics were tested in further statistical analysis. Fourier components can be considered as vectors in a Cartesian coordinate system, determined by x and y coordinates. Vectors greater than 10 μV were considered as artifacts and were excluded from further analysis. This algorithm efficiently rejected the eye blink and other artifacts. If less than 10 epochs remained after artifact rejection, which was usually the consequence of too frequent blinking, data were categorized as not available (N.A.). Signal reliability was assessed by T_{circ}^2 statistic (Victor & Mast, 1991), which analyzes the two-dimensional variances of the Fourier vectors and decides whether the average vector is significantly different than the *NULL* vector. A $p < 0.01$ significance criterion was used. This level of significance was chosen according to Victor and Mast’s (1991) suggestion because the “independent sample criteria” for the epoch length is not fully satisfied. The DRDC-VEP amplitude was defined as the double of the size of the Fourier vector at the fundamental frequency. This amplitude value corresponds to the peak to peak amplitude of the DRDC-VEP in the time domain. DRDC-VEP phases of the first harmonics were extracted from the average vectors.

Results

Subjects reported the pulsation between “woolly” depth and “snowstorm” in the DRDC stimulus at all levels including the lowest 5.5% contrast level. In the monocular red or green DRDC control trials, instead of pulsation, a homogenous “snowstorm” was perceived.

Although each subject was tested under all contrast conditions, not all subjects showed significant VEP responses in all cases. All subjects had a positive response at least for 6 different contrast levels including the fundamental, second, third, or the fourth upper harmonic frequency. After artifact rejection, at least 10 out of 35 epochs/runs remained and were used for T_{circ}^2 statistics. This analysis provided us with significant results, usually beyond $p = 0.001$, with mean $\pm \text{SEM } T_{\text{circ}}^2[2, >18] = 17.9 \pm 1.18$ for the fundamental, $T_{\text{circ}}^2 = 10.4 \pm 0.63$ for the 2nd,

Contrast	Fundamental (1st harmonic)	2nd harmonic	3rd harmonic	4th harmonic	Any	n.s.	n.a.
5.5%	10	2	2	2	11	5	0
10%	12	5	1	2	13	1	2
23%	10	7	2	7	13	3	0
30%	11	11	3	8	15	0	1
40%	12	8	3	8	15	1	0
54%	13	7	3	6	14	2	0
71%	14	3	1	6	15	1	0
80%	15	4	4	6	16	0	0
Sum	97	47	19	45	112	13	3

Table 1. Number of significant VEPs for the fundamental, second, third, and fourth harmonics of the DRDC stimulation frequency under different contrast conditions obtained from 16 individuals. The “any” means significant VEP response for any of the upper harmonics (1st–4th), “n.s.” means numbers of nonsignificant VEPs, “n.a.” means data are not available, insufficient number of epochs because of the too many blinking artifacts.

$T_{\text{circ}}^2 = 10.4 \pm 1.18$ for the 3rd harmonics, and $T_{\text{circ}}^2 = 12.8 \pm 1.05$ for the 4th harmonics. Average T_{circ}^2 values for the fundamental frequency under different stimulus contrast conditions were statistically indistinguishable at $p < 0.001$ (see Figure 2). Data were excluded from further analysis when T_{circ}^2 statistics did not prove significance. A total of 128 DRDC-VEP recordings were analyzed from

16 subjects tested under 8 conditions. From the 128 records, 112 showed significant response; 97 analyses were significant for the fundamental frequency, while 47 were significant for the 2nd, 19 for the 3rd, and 45 for the 4th upper harmonics. For details see Table 1.

Representative averaged DRDC-VEPs of subject B.R. are shown in the right side of Figure 1. The correlated and

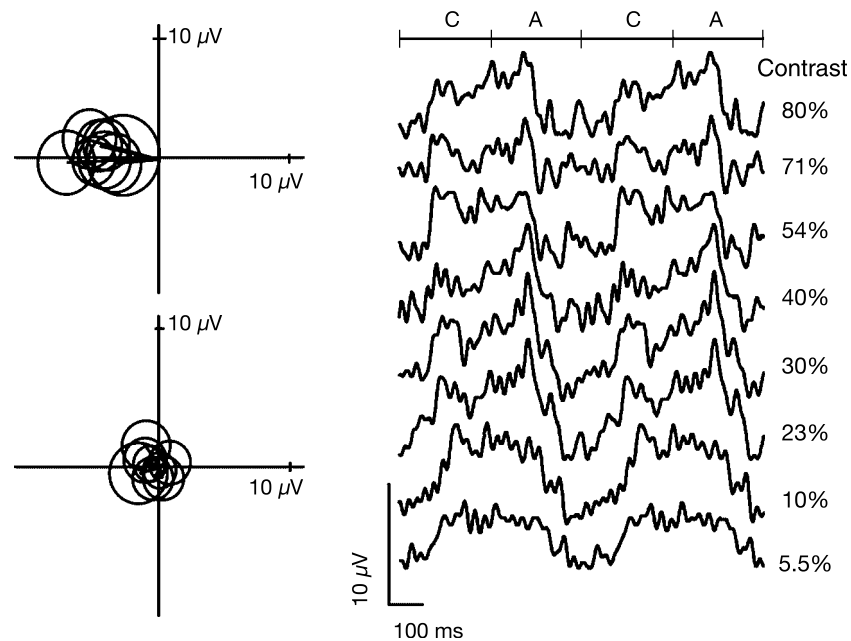


Figure 1. *Right panel*: Representative averaged dynamic random dot correlogram evoked VEPs ($n \sim 25$ epochs) of subjects B.R. DRDC-VEPs were recorded at the eight contrast levels from the highest (top trace) to the lowest (bottom trace) contrast, respectively. Letters “A” and “C” mark the anti-correlated and correlated states in DRDC stimulus. Pixel size: 7.5 min of arc; stimulus rate: 1.875 Hz; frame rate: 60 Hz. DRDCs were viewed with red-green goggles. *Top left panel*: vectographic figures of the same DRDC-VEPs. Vectors representing the Fourier components of the DRDC-VEPs belong to the stimulus fundamental frequency. The radiuses of the circles represent the confidence intervals of the average vectors at $p = 0.99$, derived from the T_{circ}^2 statistic. When the circle does not contain the origin, the DRDC-VEP fundamental frequency is phase locked to the stimulus, and it is significantly present in the EEG. *Bottom left panel*: vectographic polar plot of monocular red control DRDC-VEPs at the eight contrast level. The average vectors are NULL vectors; the stimulus has no significant effect on the EEG. The group averaged phases and amplitudes are summarized as a function of contrast in Table 2.

Contrast	<i>n</i>	Amplitude (μV)		Phase (rad)	
		Mean	SEM	Mean	SEM
5.5%	10	4.02	0.73	3.66	0.13
10%	12	4.53	0.26	3.41	0.12
23%	10	4.50	0.62	3.17	0.16
30%	11	4.73	0.40	3.15	0.14
40%	12	4.51	0.36	3.22	0.11
54%	13	4.62	0.40	3.11	0.08
71%	14	4.71	0.30	3.15	0.10
80%	15	4.48	0.39	3.21	0.09

Table 2. Amplitude and phase values of the 97 significant DRDC-VEPs for the fundamental frequency obtained from 16 individuals. The same data are plotted in Figures 2 and 3.

anti-correlated phases are marked “C” and “A.” The top left panel shows the polar plots of the mean Fourier vectors for DRDC-VEP epochs at the stimulus fundamental frequency. Circles represent the $p = 0.99$ confidence intervals around the end points of the vectors derived from T_{circ}^2 statistics. When the circle does not contain the origin, the DRDC-VEP fundamental frequency is phase locked to the stimulus, and it is significantly present in the EEG. The bottom left panel marks a vectographic polar plot of monocular red control DRDC-VEPs at the eight contrast levels. When the confidence interval—marked with the circles—contains the origin, the average vector is the NULL vector; stimulus has no significant effect on

the EEG. DRDC-VEP phases and amplitudes are summarized in numerical form in Table 2.

A linear model did not fit the observed variability in DRDC-VEP amplitudes as a function of log contrast ($F[1,95] = 0.909$; $p = 0.34$). Summary of the amplitude data for the DRDC-VEP is shown in Figure 2. The figure includes DRDC-VEPs, which showed significant T_{circ}^2 statistics at the fundamental frequency. The same analyses were performed for the other 3 upper harmonics, and all of them showed independence of contrast. We also created models which integrated amplitudes from the first (fundamental frequency) and the second and/or the third harmonics; these models showed independence of contrast as well. Results clearly indicate that the DRDC-VEP amplitude is independent of contrast.

A linear model could be fit to the phase data as a function of log contrast: $\Phi = -0.16 \times \ln(C_v) + 3.06$ ($r^2 = 0.118$, $F[1,95] = 12.75$, $p < 0.05$), where Φ is the DRDC-VEP phase in radians (see Figure 3.) and C_v is the *Michaelson contrast*. Decreased stimulus contrast lead to phase change, albeit the low r^2 has to be emphasized.

Monocular control DRDC stimulation failed to evoke a significant VEP response for each contrast level (see the monocular example in Figure 1). These results confirmed that DRDC stimuli viewed with our red or green filter alone were free from monocular cues, i.e., within channels correlated and anti-correlated frames were sufficiently balanced in luminance and contrast. A total of 88 monocular controls were sampled and none of them was

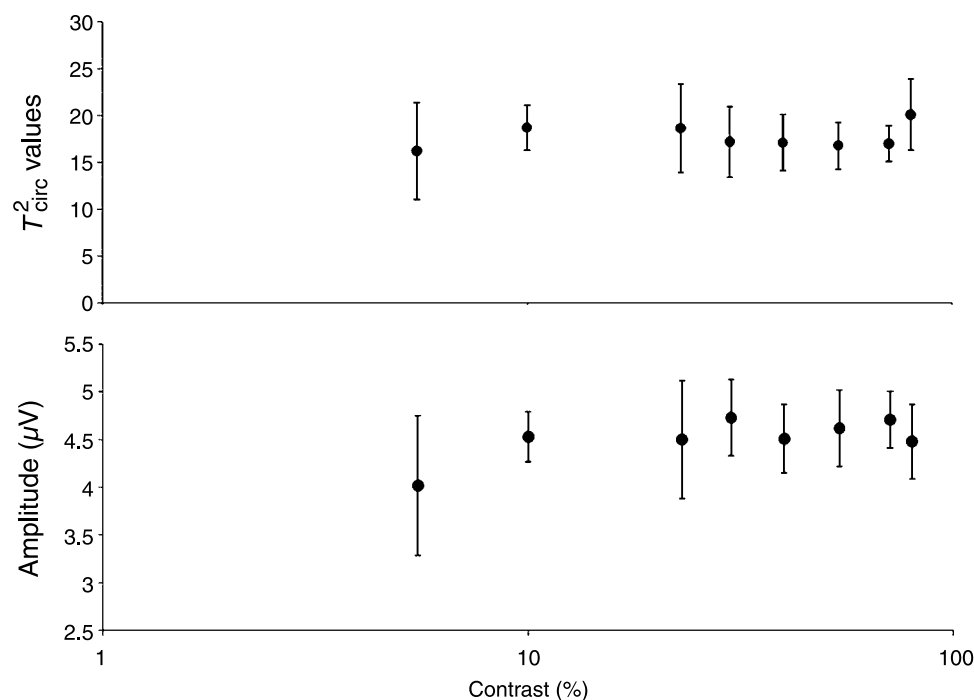


Figure 2. The T_{circ}^2 values and the CR of the DRDC-VEPs. Dots represent the group average calculated from 16 individuals, error bars represent the SEM. T_{circ}^2 values for the contrast levels from the lowest to the highest is as follows: 16(± 5), 19(± 2), 19(± 5), 17(± 4), 17(± 3), 17(± 3), 17(± 2), and 20.1(± 4). The phases and amplitudes are summarized as a function of contrast in Table 2.

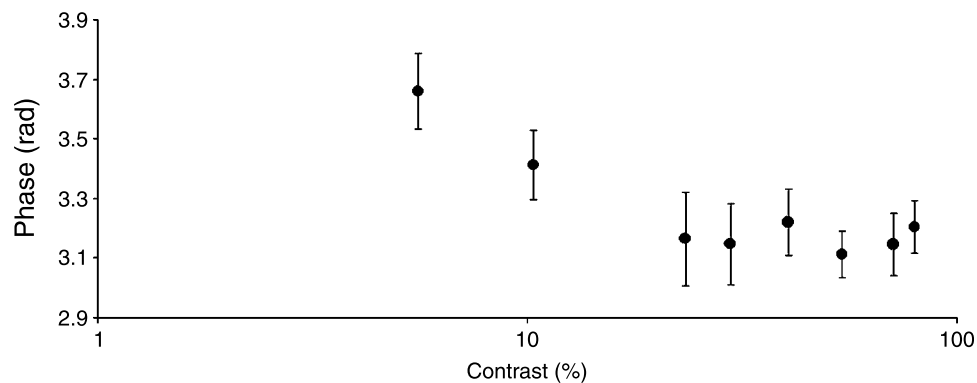


Figure 3. DRDC-VEP phases as a function of contrast. Phase: $\Phi = \arctan(y/x)$, where x and y are the decomposition of the Fourier vector of the stimulus fundamental frequency. Dots represent the group average calculated from 16 individuals, error bars represents the *SEM*.

significant, the mean $T_{\text{circ}}^2 \pm \text{SEM}$ was as follows: $T_{\text{circ}}^2 = 1.95 \pm 1.84$ for the fundamental; $T_{\text{circ}}^2 = 0.99 \pm 0.68$ for the 2nd; $T_{\text{circ}}^2 = 1.03 \pm 0.92$ for the 3rd; and $T_{\text{circ}}^2 = 0.92 \pm 0.74$ for the 4th harmonics.

Discussion

This is the first study of the contrast dependence of the DRDC-VEP. The contrast response function was flat between 5.5% and 80% contrast at a fixed mean luminance. The average T_{circ}^2 values at different stimulus contrast conditions were about the same; therefore, the detectability of the VEP response did not considerably change with stimulus contrast. A weak linear correlation was found for DRDC-VEP phase as a function of contrast.

Contrast invariance of DRDC-VEP

The contrast independent behavior observed here suggests the VEP is highly sensitive to the binocular percepts with DRDC; however, the responses are nonlinear and saturate at low contrast levels. The response did not show contrast gain within the attainable range, i.e., the initial part with the steep slope in the CR was missing (Figure 2). There are two possible explanations for this: (1) the high contrast gain could be found somewhere below 5.5%, which was out of the attainable range of this study due to technical limitations. (2) Contrast gain cannot be detected with our method at all. Conceivably, if contrast was further decreased, DRDC amplitude and thus detectability would decline in parallel. The CR of the DRDC-VEP did not show evidence of multiple contrast mechanisms (i.e., the CR did not have multi-slope characteristics) either, which was often seen in CRs of contrast evoked VEPs (Rudvin et al., 2000; Souza et al., 2007; Valberg & Rudvin, 1997). In summary, the invariance of DRDC-VEP amplitude is actually the saturated (i.e., leveling off) part of a nonlinear CR, involving a

single contrast sensitivity mechanism. It is noteworthy that the detectability of the response was also independent of contrast down to the lowest 5.5% contrast and only 5 out of 16 subjects failed to show significant DRDC-VEP at the lowest contrast. A slight increase of nonsignificant responses occurs at the inflection point of the CR.

A change in the VEP phase is due to changes in response timing. Although the real response time is difficult to determine, the change in phase has been associated with elongation of neuronal processing time (Regan, 1988). A weak linear correlation was found for DRDC-VEP phase as a function of contrast. The weak correlation can be explained by the nonlinear characteristics of the response. The phase was constant within the 23–80% contrast range; it gradually changed at the two lowest contrasts only. At the neuronal level, lower contrast most probably increases the integration time of binocular information.

Random dot images, built up from pixels, have a composite spatial frequency spectrum. All spatial wavelengths from twice of the pixel size to the entire screen width (corresponding to 0.05–4 cycles/degree) are present at the same time roughly with equal power. The element size, which is the limiting parameter for the highest spatial frequency, was equal to the smallest found in the literature.

Parallel visual pathways and DRDC-VEP

The notion of two functionally and anatomically segregated parallel visual pathways (i.e., MC and PC pathways) that extend from the retina to the higher visual cortical areas was an influential and widely accepted model in neuroscience shortly after it appeared (Livingstone & Hubel, 1987; Maunsell, 1987). Research testing this functional division over the years has provided a strong basis for modifying this model. In particular, the correspondence between the cortical and subcortical pathways has to be reconsidered. Intermixing of MC and PC pathways is apparent in V1 and V2 (Malpeli, Schiller, & Colby, 1981), the first levels a cortical processing, and if it

continues at later stages, the pathways would reflect not differential MC and PC contribution, but differences in the way that a combined signal is processed (Merigan & Maunsell, 1993).

The flat CR in our study suggests the contribution of a single contrast-sensitivity mechanism in the generation of DRDC-VEP. Since the high contrast gain and quick saturation of the firing rate at low contrast are the properties of the MC neurons, the flat CR is likely to be due to the involvement of the MC pathway in the correlation processing system. However, we must emphasize that the shared sensitivities of the observed DRDC-VEP and the MC neurons do not establish that the two sensitivities stem from a common pathway. This could be verified by selective lesions of the PC or MC pathways in experimental animals.

Recently, there is an increasing clinical demand for electrophysiological tools to studying the integrity of MC and PC visual pathway separately. Several authors claim selective or dominant impairment of MC system in retinitis pigmentosa (Alexander et al., 2005), schizophrenia (Martinez et al., 2008), glaucoma (Klistorner & Graham, 1999), and dyslexia (Stein, 2001). It would be interesting to study the CR of the DRDC-VEP in the above patients. If selective impairment of the MC pathway in such patients decreased the contrast gain in the CR, it would be further support a dominant role of the MC pathway in generating the DRDC-VEP.

Technical considerations

A disadvantage of the anaglyphic technique is its limited luminance range and the relative complexity of the luminance calibration (for monitor calibration, see Appendix A).

There are several other stereoscopic techniques that are free from the above disadvantages; however, we would like to comment that the technique employed here has a number of advantages over the others.

1. We used goggles with red and green filters in order to provide the best possible separation between the left and right eyes. There have also been attempts to use red-blue color channels (Birch & Petrig, 1996). Although red-blue cyclopean stimuli provide less crosstalk compared to red-green ones, using red-green channels may be more advantageous, because the blue dots are mainly processed by the S-cones which are quite different in many respects (anatomical connections, distribution in the retina, visual acuity, temporal resolution) from the L-M-cones (Calkins, 2001).
2. The anaglyph goggles that we used seem to be more effective than time-multiplexed frames presented through liquid crystal shutters (Eizenman et al., 1999; Westall et al., 1998). The problem with the shutters is that the two images for the left and the right eyes are never present at the same time on

the two retinas. Because of the time-multiplexed presentation of the two channels, the simultaneous perception and fusion is based on retinal afterimages. In addition, alternating blackout of the two sides introduces an unnecessary luminance artifact at the frequency of the frame rate.

3. Stereoscopes, including head mounted binocular LCD video goggles (Engström, Ragnehed, & Lundberg, 2005), have the advantages of perfect channel separation and the additionally available color information. The major disadvantage of this device is that images are more difficult to fuse for the subjects, and the fusion is hard to verify. In addition, the use of these devices is limited to well-cooperating adult subjects. The critical disadvantage of LCDs over CRT devices in dynamic stimulation is that LCDs have an asynchronous image updating mechanism. Because of that, it is impossible to synchronize image change to the monitor refresh cycle, and there will be more variability in the electrophysiological measurements.

The given 8 bits/chromatic channel graphic adaptor did not allow us to study DRDC-VEPs at lower than 5.5% contrasts.

Conclusion

Although the DRDC-VEP was invented 3 decades ago, the fundamental parameters of the method of stimulation have never been examined systematically. The effects of stimulus parameters, including contrast, on the DRDC-VEP response and the cerebral processing mechanisms of the stimulus have not been clarified before. Our results clearly demonstrated that there is no significant correlation between DRDC-VEP amplitude and stimulus contrast in our conditions. DRDC-VEP can be evoked in a wide range of contrast (~5%–80%) conditions in adults without compromising detectability of the response. Contrast independence refers to high contrast gain for DRDC-VEP response, which is saturated at or below 5% contrast. Such a CR of the DRDC-VEP suggests a dominant MC input to the neuronal processing mechanism of binocular correlation.

Appendix A

Dynamic random dot stereogram with Snellen E (DRDS-E)

DRDS-Es were generated on a personal computer with a custom made direct-X-based Windows utility and

presented on a 19-inch CRT monitor. Each frame in the DRDS-E had an anaglyphic red-green random dot stereogram with a Snellen E figure in one of the four orientations (i.e., left, right, up, or down). Images were composed of 50% dark and 50% bright dots. One dot in the DRDS-E subtended 1.6 min of arc, the whole Snellen E figure was visible at 160 min of arc and the horizontal crossed disparity, introduced in the stereogram, was 0.8 min of arc from the 1-m viewing distance. Random dot stereogram frames were updated at 60 Hz. The image change was synchronized to the monitor refresh cycle. DRDS-E was free of monocular cues; therefore, the orientation of the figures could not be determined either through the red or the green filter alone. To pass the test, the subject had to determine the orientation of 4 randomly generated DRDS-Es within a 20-s time limit. In general, strabismic or amblyopic patients are not able to pass this test.

Red and green filters

Red and green filters were specifically developed for viewing red-green DRDC and DRDS stimuli presented on a CRT monitor. The red filter transmitted <0.5% at 565 nm, 50% at 612 nm, and 89% at 700 nm. The band-pass green filter transmitted <0.5% at 458 nm and at 585 nm; the peak transmission was 29% at 519 nm.

Monitor calibration

Luminance measurements were made by two independent methods: (1) Spectrocam 75 RE spectrophotometer (Avantes Inc., Eerbeek, Netherlands) with a computerized method (Samu, 2002). (2) Photometric measurement at each RGB level for each filter respectively (IL-1700 Photometer, International Light Technologies, Peabody, USA). Although the two measurements were similar, we used the photometric data, since they were real measurements instead of a function based approximation.

Due to the complex nature of the DRDC stimulus, the potential sources of monocular artifacts are numerous. At least four luminance and four contrasts have to remain constant at the same time to avoid monocular artifacts: the contrasts and space-average mean luminance of the (1) correlated and the (2) anti-correlated frames within the (3) left and (4) right channels have to be equal within an acceptable range.

The best RGB values for each contrast level were calculated by an iterative least square algorithm. The free parameters of the model were the 4 red and green monitor gun value pairs to be used in the black, yellow, red, and green pixels of the DRDC stimulus. The model calculated the luminance and contrast of the stimulus taking into account the residual transmission of the filters and

response nonlinearity (gamma) of the monitor as measured through the red and green filters of the goggles. The summed squared error between the actual and the desired contrast plus the actual and the desired luminance was then minimized using gradient descent optimization algorithm. Best fit parameter values yielded less than 5% error relative to the desired luminance and contrast for any of the 6 highest contrasts and less than 10% for the lower 2 contrasts used.

The resulting best RGB combinations were photometrically controlled and psychophysically tested. DRDS-Es were generated with the same RGB combinations and viewed monocularly through red or green filters, respectively. Slight adjustments were made if required to avoid monocular cues in the stimulus.

For electrophysiological control, monocular DRDC stimulation through the red filter (the other eye covered), DRDC stimulation through the green filter (the other eye covered) were performed. Control conditions tested the absence of monocular electrical response, which might have resulted in false DRDC-VEPs. Each DRDC control run was sampled for the same 70-s duration as binocular stimulation. Subjects were asked to fixate at the center of the monitor, to avoid body movements, and to report their perception between the runs. Controls were not performed at all contrasts but at least at two randomly selected contrast levels for each subject. In cases of the two subjects, controls were made for each contrast respectively. In the monocular conditions, subjects were not able to identify transition between the phases of DRDC stimulus at any contrast.

Animation of DRDC stimulus

An example movie of the DRDC stimulus is shown in the QuickTime format. Red-green or red-blue goggles should be used for viewing the stimulus. The frame rate is set to 30 Hz, and the resolution is 50×50 pixels. If the movie is played at the right frame rate, the stimulus frequency is 0.5 Hz. At this stimulus rate, the correlated phase provides the percept of a noisy surface, while during the anti-correlated phase “wooly depth” is perceived. Some individuals describe the anti-correlated phase as “a hole in the monitor.” In our experiment, the frame rate was 60 Hz; stimulus frequency was 1.875 Hz.

Acknowledgments

We thank Prof. László Lénárd for his comprehensive support and Heather Read for her valuable scientific critiques to improving English style and grammatical corrections. We also thank Péter Buzás, Richárd Tobiás, Lóránd Kelényi, Csaba Niedetzky, László Závori, and

staff members of the Institute of Physiology University of Pécs Medical School for their contribution. This work was supported by the Hungarian Academy of Science and by OTKA-NF-60806 to I.K. The principal investigator in this study was G. J.

Commercial relationships: none.

Corresponding author: Gábor Jandó.

Email: gabor.jando@aok.pte.hu.

Address: Institute of Physiology, Medical School University of Pécs, 12. Szigeti str. H-7624 Pécs, Hungary.

References

- Alexander, K. R., Rajagopalan, A. S., Seiple, W., Zemon, V. M., & Fishman, G. A. (2005). Contrast response properties of magnocellular and parvocellular pathways in retinitis pigmentosa assessed by the visual evoked potential. *Investigative Ophthalmology & Visual Science*, *46*, 2967–2973. [[PubMed](#)] [[Article](#)]
- Birch, E., & Petrig, B. (1996). FPL and VEP measures of fusion, stereopsis and stereoacuity in normal infants. *Vision Research*, *36*, 1321–1327. [[PubMed](#)]
- Bobak, P., Bodis-Wollner, I., Harnois, C., & Thornton, J. (1984). VEPs in humans reveal high and low spatial contrast mechanisms. *Investigative Ophthalmology & Visual Science*, *25*, 980–983. [[PubMed](#)] [[Article](#)]
- Braddick, O., Atkinson, J., Julesz, B., Kropfl, W., Bodis-Wollner, I., & Raab, E. (1980). Cortical binocularity in infants. *Nature*, *288*, 363–365. [[PubMed](#)]
- Calkins, D. J. (2001). Seeing with S cones. *Progress in Retinal and Eye Research*, *20*, 255–287. [[PubMed](#)]
- Campbell, F. W., & Maffei, L. (1970). Electrophysiological evidence for the existence of orientation and size detectors in the human visual system. *The Journal of Physiology*, *207*, 635–652. [[PubMed](#)] [[Article](#)]
- Cormack, L. K., Stevenson, S. B., & Schor, C. M. (1991). Interocular correlation, luminance contrast and cyclopean processing. *Vision Research*, *31*, 2195–2207. [[PubMed](#)]
- den Ouden, H. E., van Ee, R., & de Haan, E. H. (2005). Colour helps to solve the binocular matching problem. *The Journal of Physiology*, *567*, 665–671. [[PubMed](#)] [[Article](#)]
- Eizenman, M., Westall, C. A., Geer, I., Smith, K., Chatterjee, S., Panton, C. M., et al. (1999). Electrophysiological evidence of cortical fusion in children with early-onset esotropia. *Investigative Ophthalmology & Visual Science*, *40*, 354–362. [[PubMed](#)] [[Article](#)]
- Engström, M., Ragnehed, M., & Lundberg, P. (2005). Projection screen or video goggles as stimulus modality in functional magnetic resonance imaging. *Magnetic Resonance Imaging*, *23*, 695–699. [[PubMed](#)]
- Halpern, D. L., & Blake, R. R. (1988). How contrast affects stereoacuity. *Perception*, *17*, 483–495. [[PubMed](#)]
- Julesz, B., Kropfl, W., & Petrig, B. (1980). Large evoked potentials to dynamic random-dot correlograms and stereograms permit quick determination of stereopsis. *Proceedings of the National Academy of Sciences of the United States of America*, *77*, 2348–2351. [[PubMed](#)] [[Article](#)]
- Kaplan, E., & Shapley, R. M. (1982). X and Y cells in the lateral geniculate nucleus of macaque monkeys. *The Journal of Physiology*, *330*, 125–143. [[PubMed](#)] [[Article](#)]
- Klistorner, A. I., & Graham, S. L. (1999). Early magnocellular loss in glaucoma demonstrated using the pseudorandomly stimulated flash visual evoked potential. *Journal of Glaucoma*, *8*, 140–148. [[PubMed](#)]
- Legge, G. E., & Gu, Y. C. (1989). Stereopsis and contrast. *Vision Research*, *29*, 989–1004. [[PubMed](#)]
- Lehmann, D., & Julesz, B. (1978). Lateralized cortical potentials evoked in humans by dynamic random-dot stereograms. *Vision Research*, *18*, 1265–1271. [[PubMed](#)]
- Livingstone, M. S., & Hubel, D. H. (1987). Psychophysical evidence for separate channels for the perception of form, color, movement, and depth. *Journal of Neuroscience*, *7*, 3416–3468. [[PubMed](#)] [[Article](#)]
- Malpeli, J. G., Schiller, P. H., & Colby, C. L. (1981). Response properties of single cells in monkey striate cortex during reversible inactivation of individual lateral geniculate laminae. *Journal of Neurophysiology*, *46*, 1102–1119. [[PubMed](#)]
- Martinez, A., Hillyard, S. A., Dias, E. C., Hagler, D. J., Jr., Butler, P. D., Guilfoyle, D. N., et al. (2008). Magnocellular pathway impairment in schizophrenia: Evidence from functional magnetic resonance imaging. *Journal of Neuroscience*, *28*, 7492–7500. [[PubMed](#)] [[Article](#)]
- Maunsell, J. H. R. (1987). Physiological evidence for two visual subsystems. In L. Vaina (Ed.), *Matters of intelligence* (pp. 59–87). Dordrecht: Reidel.
- Merigan, W. H., & Maunsell, J. H. (1993). How parallel are the primate visual pathways? *Annual Review of Neuroscience*, *16*, 369–402. [[PubMed](#)]
- Miezin, F. M., Myerson, J., Julesz, B., & Allman, J. M. (1981). Evoked potentials to dynamic random-dot correlograms in monkey and man: A test for cyclopean perception. *Vision Research*, *21*, 177–179. [[PubMed](#)]
- Morale, S. E., Jeffrey, B. G., Fawcett, S. L., Stager, D. R., Salomão, S. R., Berezovsky, A., et al. (2002).

- Preschool Worth 4-Shape test: Testability, reliability, and validity. *Journal of AAPOS*, 6, 247–251. [[PubMed](#)]
- Odom, J. V., Bach, M., Barber, C., Brigell, M., Marmor, M. F., Tormene, A. P., et al. (2004). Visual evoked potentials standard (2004). *Documenta Ophthalmologica*, 108, 115–123. [[PubMed](#)]
- Petrig, B., Julesz, B., Kropfl, W., Baumgartner, G., & Anliker, M. (1981). Development of stereopsis and cortical binocularity in human infants: Electrophysiological evidence. *Science*, 213, 1402–1405. [[PubMed](#)]
- Regan, D. (1988). Human event related potentials. In T. W. Picton (Ed.), *EEG handbook* (vol. 3, pp. 159–243). New York: Oxford Elsevier Science Publishers.
- Rudvin, I., Valberg, A., & Kilavik, B. E. (2000). Visual evoked potentials and magnocellular and parvocellular segregation. *Visual Neuroscience*, 17, 579–590. [[PubMed](#)]
- Samu, K. (2002). Automatized gamma-curve measurement of CRT computer monitors. *Gépészet*, 817–821.
- Shapley, R., Kaplan, E., & Soodak, R. (1981). Spatial summation and contrast sensitivity of X and Y cells in the lateral geniculate nucleus of the macaque. *Nature*, 292, 543–545. [[PubMed](#)]
- Smith, E. L., III, Chino, Y., Ni, J., & Cheng, H. (1997). Binocular combination of contrast signals by striate cortical neurons in the monkey. *Journal of Neurophysiology*, 78, 366–382. [[PubMed](#)] [[Article](#)]
- Souza, G. S., Gomes, B. D., Saito, C. A., da Silva Filho, M., & Silveira, L. C. (2007). Spatial luminance contrast sensitivity measured with transient VEP: Comparison with psychophysics and evidence of multiple mechanisms. *Investigative Ophthalmology & Visual Science*, 48, 3396–3404. [[PubMed](#)] [[Article](#)]
- Stein, J. (2001). The magnocellular theory of developmental dyslexia. *Dyslexia*, 7, 12–36. [[PubMed](#)]
- Stevenson, S. B., & Cormack, L. K. (2000). A contrast paradox in stereopsis, motion detection, and vernier acuity. *Vision Research*, 40, 2881–2884. [[PubMed](#)]
- Valberg, A., & Rudvin, I. (1997). Possible contributions of magnocellular- and parvocellular-pathway cells to transient VEPs. *Visual Neuroscience*, 14, 1–11. [[PubMed](#)]
- Victor, J. D., & Mast, J. (1991). A new statistic for steady-state evoked potentials. *Electroencephalography and Clinical Neurophysiology*, 78, 378–388. [[PubMed](#)]
- Westall, C. A., Eizenman, M., Kraft, S. P., Panton, C. M., Chatterjee, S., & Sigesmund, D. (1998). Cortical binocularity and monocular optokinetic asymmetry in early-onset esotropia. *Investigative Ophthalmology & Visual Science*, 39, 1352–1360. [[PubMed](#)] [[Article](#)]
- Worth, C. (1903). *Squint: Its causes, pathology, and treatment*. Philadelphia: Blakiston.